

# High-Index-Facet Metal-Alloy Nanoparticles as Fuel Cell Electrocatalysts

*Liliang Huang, Cindy Y. Zheng, Bo Shen, and Chad A. Mirkin\**

L. Huang, Prof. C. A. Mirkin  
Department of Materials Science and Engineering  
Northwestern University  
2220 Campus Drive, Evanston, IL 60208, USA  
E-mail: chadnano@northwestern.edu

C. Y. Zheng, Dr. B. Shen, Prof. C. A. Mirkin  
Department of Chemistry  
Northwestern University  
2145 Sheridan Road, Evanston, IL 60208, USA

Prof. C. A. Mirkin  
International Institute for Nanotechnology  
Northwestern University  
2145 Sheridan Road, Evanston, IL 60208, USA

 The ORCID identification number(s) for the author(s) of this article can be found under <https://doi.org/10.1002/adma.202002849>.

**DOI: 10.1002/adma.202002849**

Spoorthi  
27/06/2020

# Background

## Engineered Graphene Materials: Synthesis and Applications for Polymer Electrolyte Membrane Fuel Cells

*Daping He, Haolin Tang,\* Zongkui Kou, Mu Pan, Xueliang Sun, Jiujuun Zhang, and Shichun Mu\**

*Adv. Mater.* **2017**, 1601741

## Nanoporous bimetallic Pt–Au alloy nanocomposites with superior catalytic activity towards electro-oxidation of methanol and formic acid†

*Zhonghua Zhang,\*<sup>a</sup> Yan Wang\*<sup>b</sup> and Xiaoguang Wang<sup>a</sup>*

*Received 5th November 2010, Accepted 1st January 2011*

DOI: 10.1039/c0nr00830c

# Sub-4 nm PtZn Intermetallic Nanoparticles for Enhanced Mass and Specific Activities in Catalytic Electrooxidation Reaction

Zhiyuan Qi,<sup>†</sup> Chaoxian Xiao,<sup>†</sup> Cong Liu,<sup>‡</sup> Tian Wei Goh,<sup>†, </sup> Lin Zhou,<sup>§</sup> Raghu Maligal-Ganesh,<sup>†</sup>  
Yuchen Pei,<sup>†</sup> Xinle Li,<sup>†</sup> Larry A. Curtiss,<sup>||, </sup> and Wenyu Huang<sup>\*, †, §, </sup>

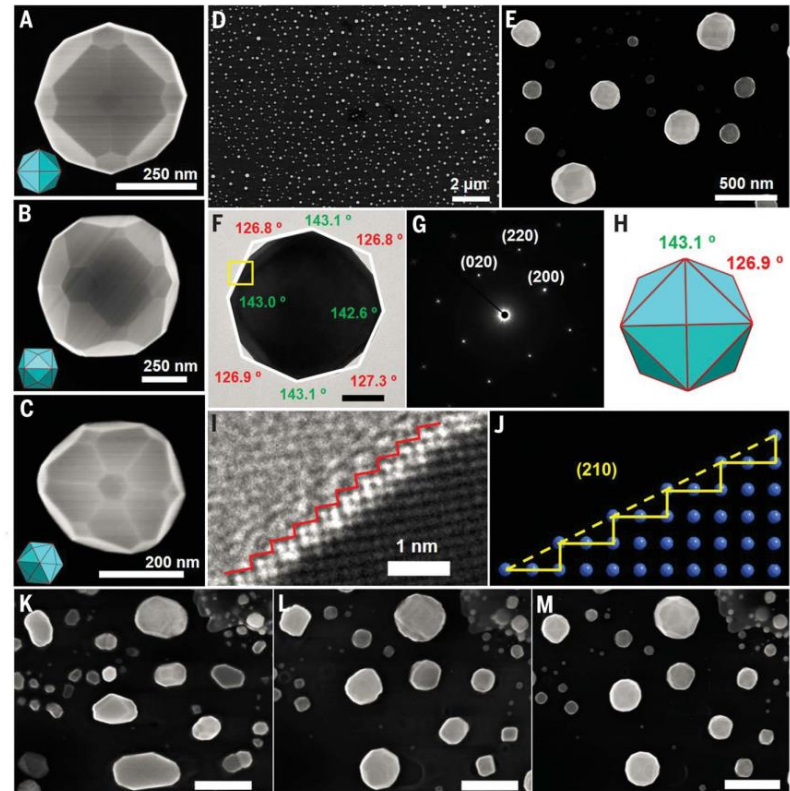
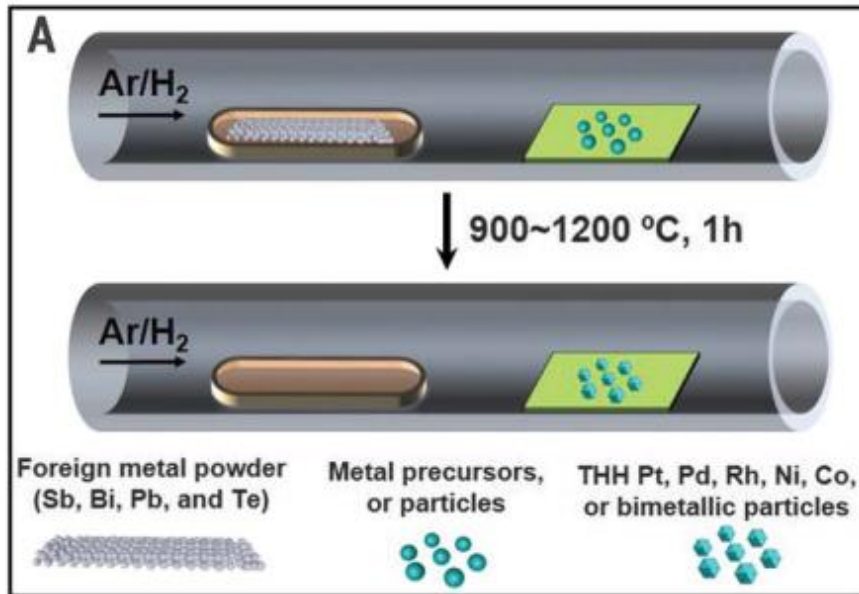
J. Am. Chem. Soc. 2017, 139, 4762-4768

# Multimetallic High-Index Faceted Heterostructured Nanoparticles

Liliang Huang, Haixin Lin, Cindy Y. Zheng, Edward J. Kluender, Rustin Golnabi, Bo Shen,  
and Chad A. Mirkin<sup>\*</sup>

# Shape regulation of high-index facet nanoparticles by dealloying

Liliang Huang<sup>1</sup>, Mohan Liu<sup>1</sup>, Haixin Lin<sup>2,3</sup>, Yaobin Xu<sup>1</sup>, Jinsong Wu<sup>1</sup>,  
Vinayak P. Dravid<sup>1,2</sup>, Chris Wolverton<sup>1</sup>, Chad A. Mirkin<sup>1,2,3\*</sup>



# Introduction

- ❑ They have synthesized a series of Pt–M (M = Co, Ni, and Cu) and Rh–M (M = Ni and Co) THH alloy NPs through Bi modification.
- ❑ Systematically explored their catalytic efficiencies and stabilities toward several fuel cell reactions—the electrooxidations of formic acid, methanol, and ethanol.
- ❑ Their performances were compared with those of both commercial Pt and Rh catalysts to understand the relative importance of
  - High-index facets
  - Alloying with transition metal elements
  - Surface Bi modification

# Synthesis of THH nanoparticles

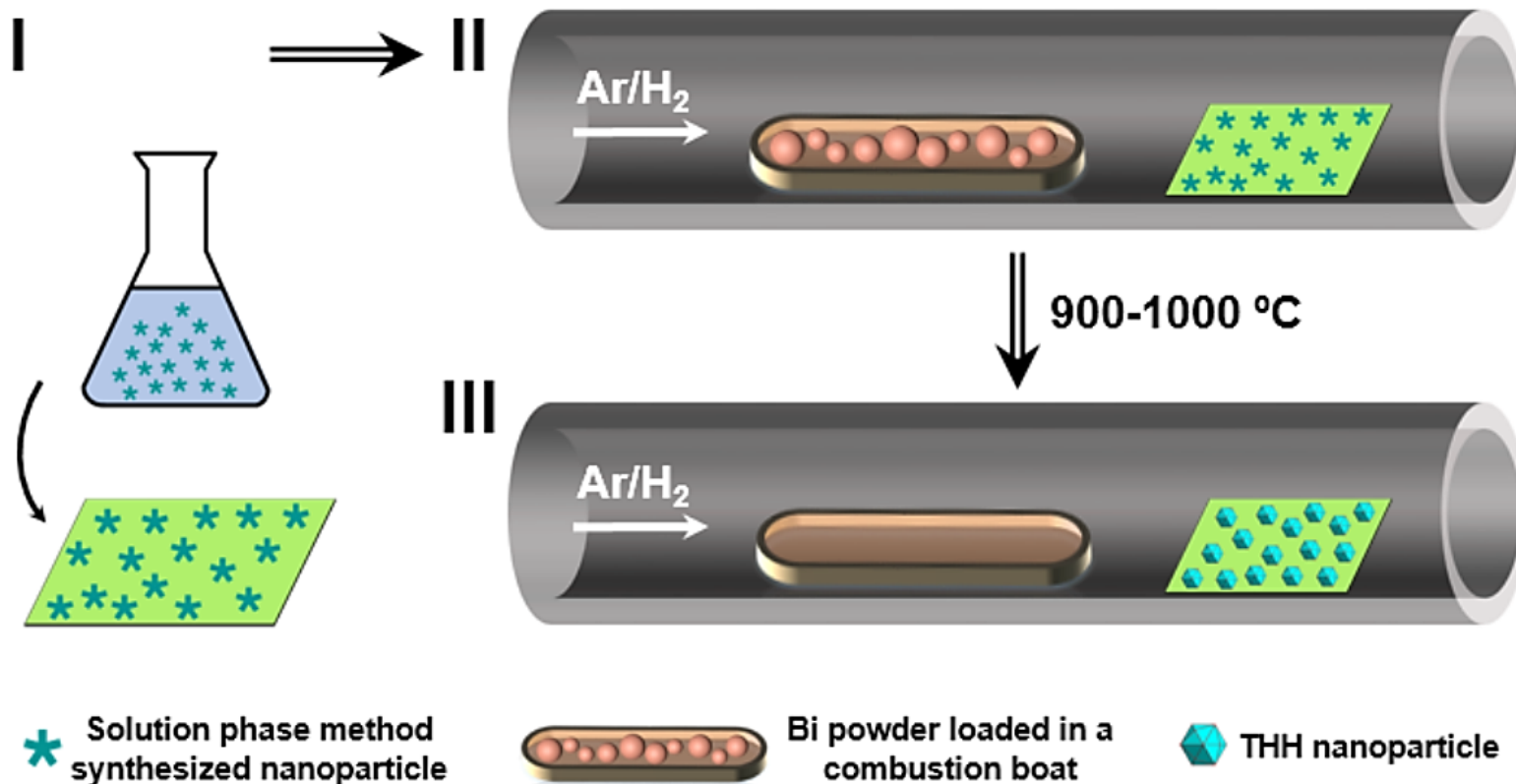


**Figure S1.** Scheme for synthesizing compositionally uniform THH nanoparticles. (I) Uniform nanoparticles were synthesized via a solution-phase method and were loaded onto a catalyst support. (II) Approximately 1 mg of Bi powder was loaded in a combustion boat, which was then transferred to a tube furnace. The nanoparticle-loaded support was placed downstream of the Bi powder. (III) After thermal treatment in an Ar/H<sub>2</sub> atmosphere, the Bi powder was completely transferred to the nanoparticles via evaporation and THH nanoparticles formed.

# Characterizations

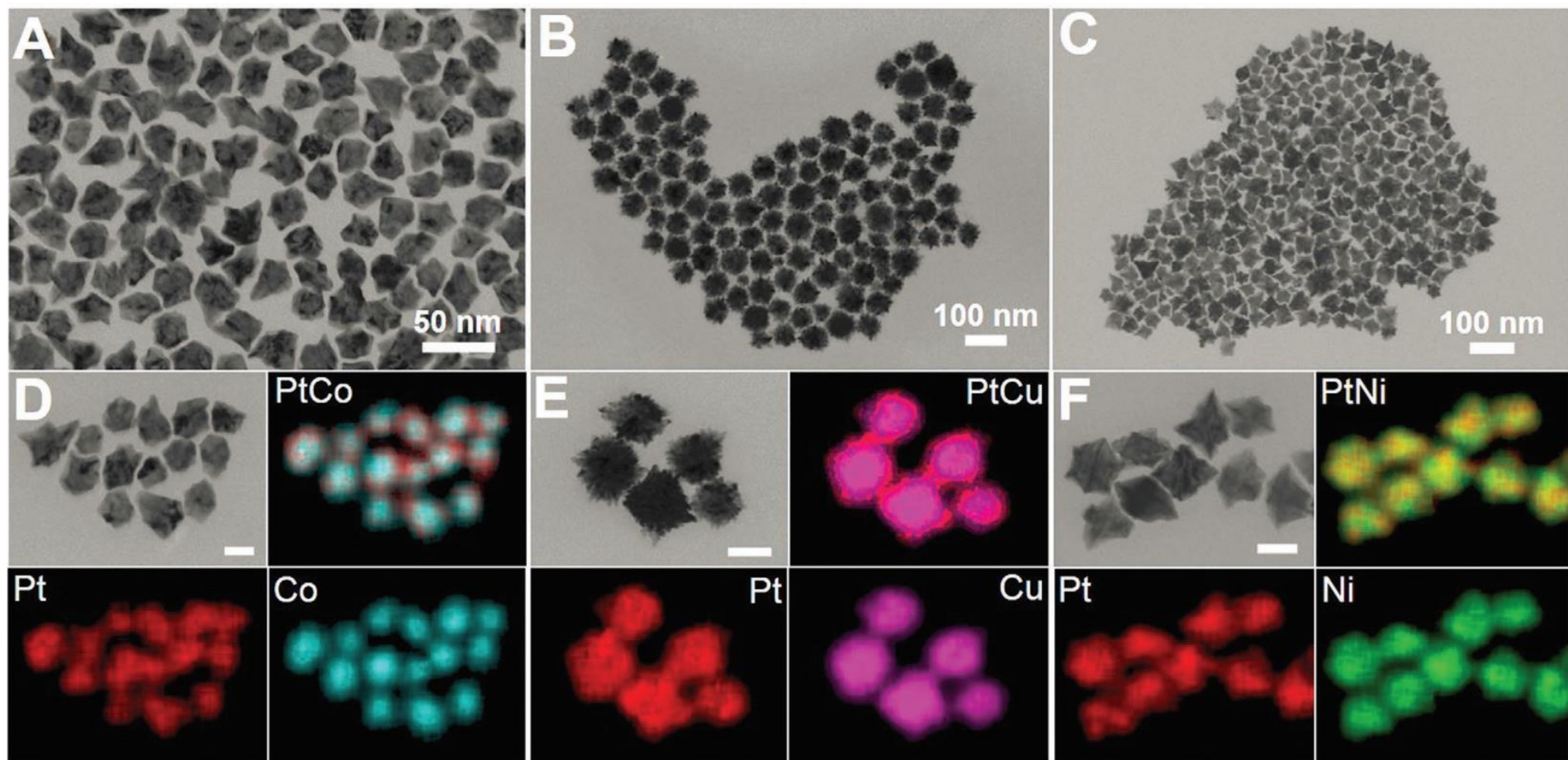


**Figure 1.** A–C) Scanning transmission electron microscopy (STEM) images of colloidal PtCo (55% Pt, 45% Co) (A), PtCu (41% Pt, 59% Cu) (B), and PtNi (45% Pt, 55% Ni) (C) nanoparticles. D–F) High-magnification STEM images and corresponding EDS elemental maps of PtCo (D), PtCu (E), and PtNi (F) nanoparticles. Scale bars: 20 nm in (D), 50 nm in (E), and 30 nm in (F).

# Characterizations

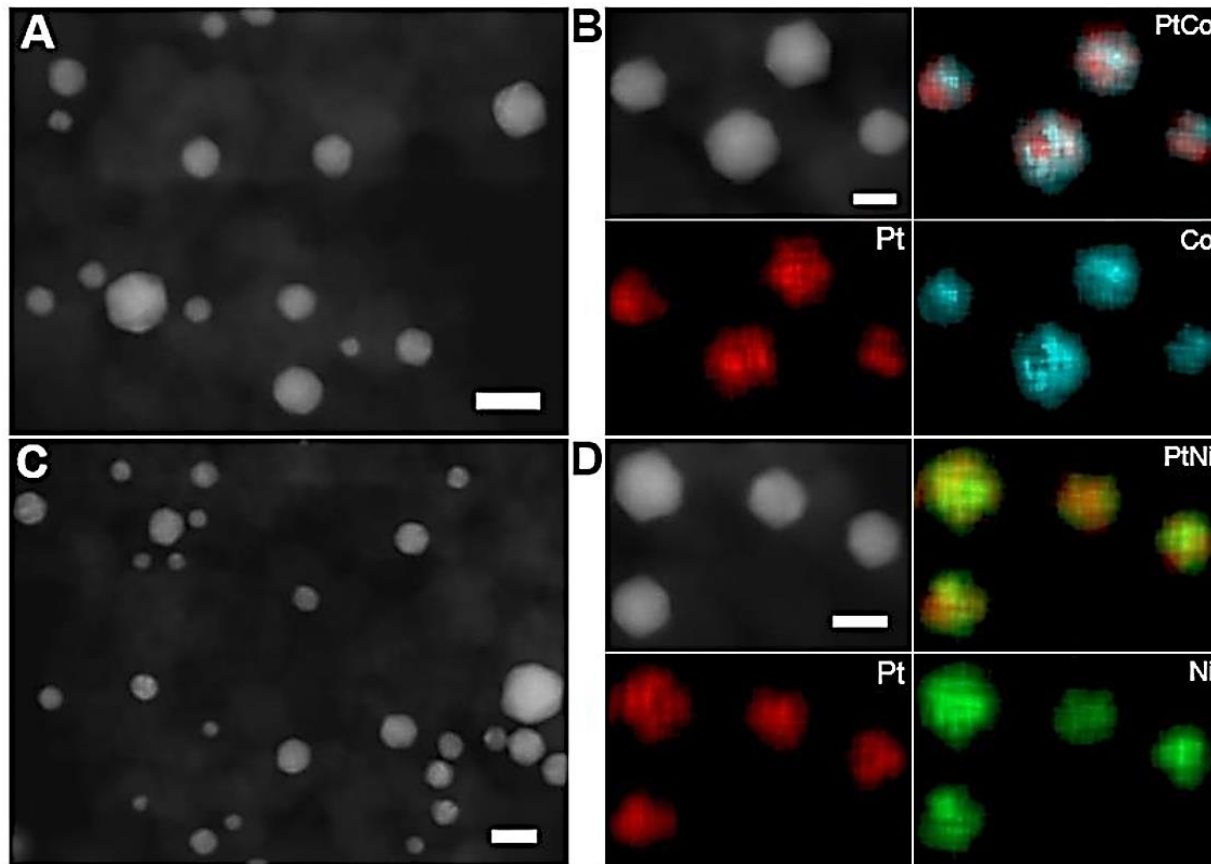


**Figure S4.** (A) STEM image of PtCo THH nanoparticles loaded on carbon black powder. (B) STEM image and corresponding EDS elemental maps of PtCo THH nanoparticles. (C) STEM image of PtNi THH nanoparticles loaded on carbon black powder. (D) STEM image and corresponding EDS elemental maps of PtNi THH nanoparticles. Scale bars: 50 nm in (A) and (C), 25 nm in (B), and 30 nm in (D)

# Characterizations

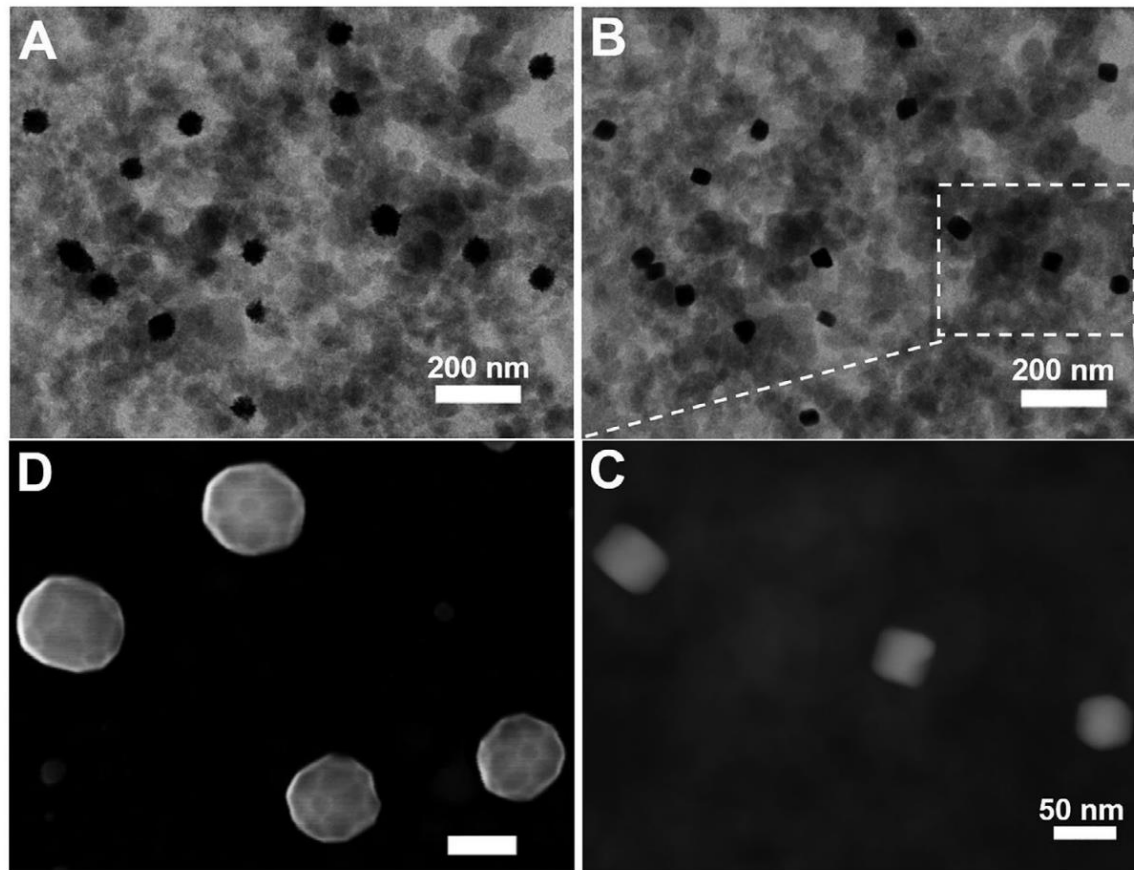


**Figure 2.** A,B) Bright-field STEM images of as-synthesized colloidal PtCu nanoparticles loaded on carbon black powder (A) and THH PtCu nanoparticles (B) in the same area as (A) after treating sample (A) at 900 °C for 1 h with  $\approx 1$  mg of Bi powder. As-synthesized colloidal PtCu nanoparticles exhibit a quasi-spherical shape with a spiky surface while THH PtCu nanoparticles show a cubic-like morphology in the STEM images. C) Dark-field STEM image of PtCu THH nanoparticles in the boxed area in (B). D) Scanning electron microscopy (SEM) image of THH PtCu nanoparticles synthesized on a Si wafer.

# Electrochemical measurements

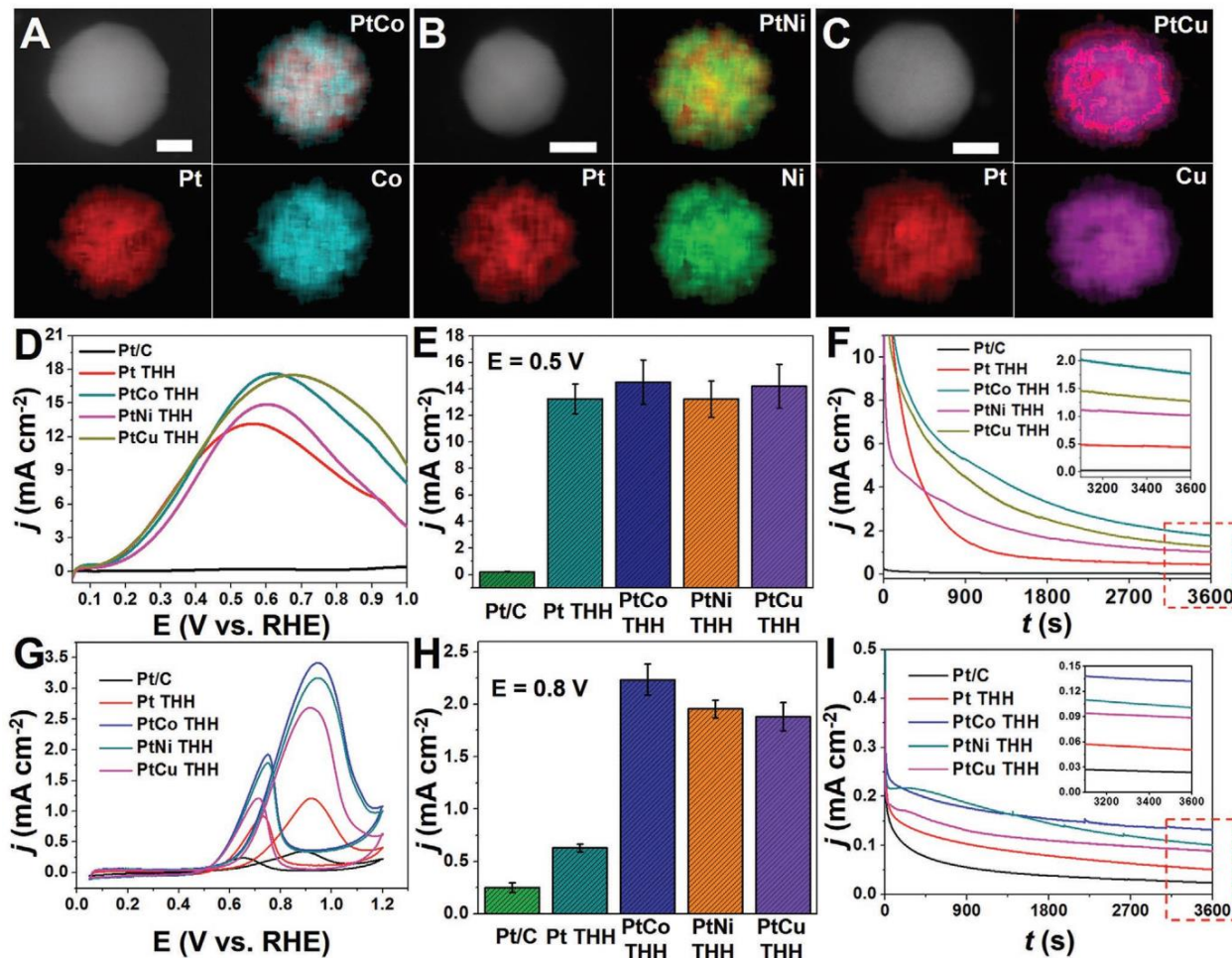


**Figure 3.** A–C) STEM images and corresponding elemental maps of PtCo (A), PtNi (B), and PtCu (C) THH nanoparticles. D) Polarization curves and E) histograms of the specific activities at 0.5 V of formic acid electrooxidation for different catalysts in Ar-saturated 0.5 m HCOOH + 0.5 m H<sub>2</sub>SO<sub>4</sub>. F) Chronoamperometry curves of formic acid electrooxidation for the different catalysts at 0.5 V. G) Polarization curves and H) histograms of the specific activities at 0.8 V of methanol electrooxidation in Ar-saturated 0.5 m H<sub>2</sub>SO<sub>4</sub> + 1 m CH<sub>3</sub>OH for different catalysts. I) Chronoamperometry curves of methanol electrooxidation for the different catalysts at 0.8 V. Error bars in (E) and (H) represent the standard deviation. Scale bars: 20 nm

# Electrochemical measurements

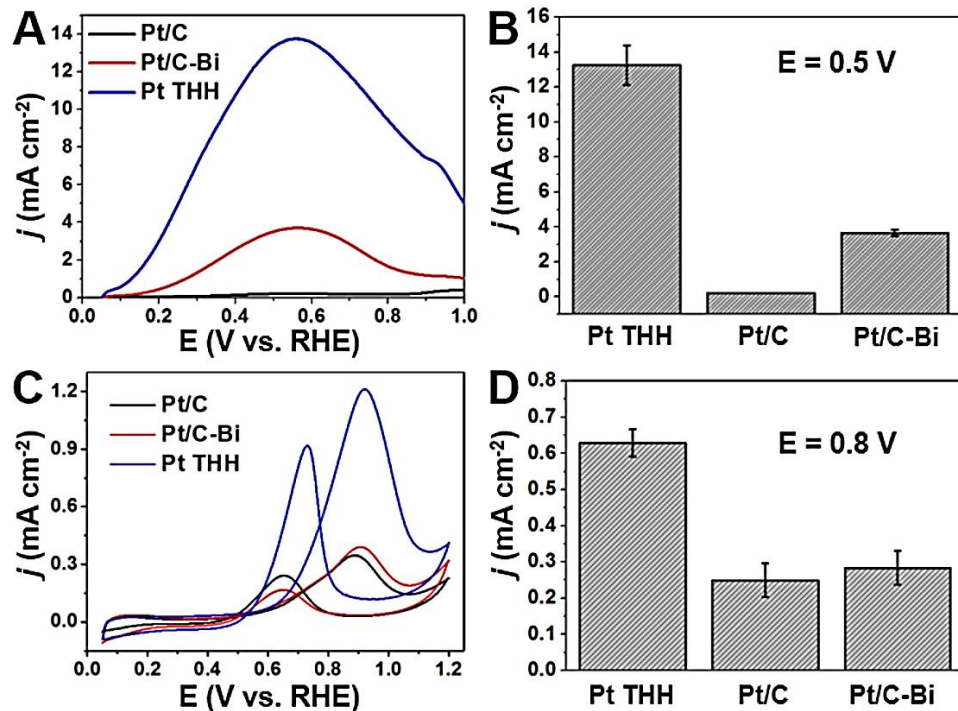
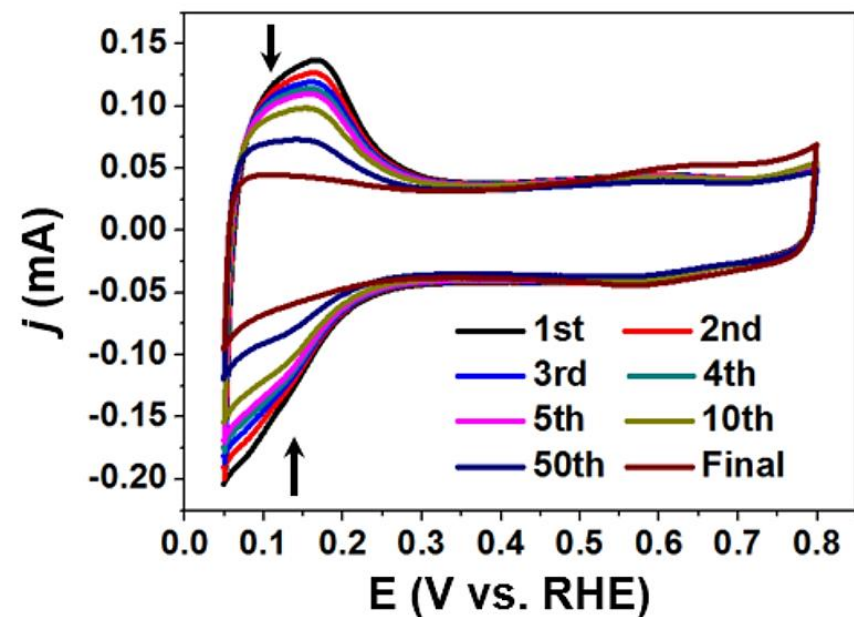


**Figure S9.** Cyclic voltammograms illustrating the Bi decoration process on a commercial Pt/C catalyst. The arrows point to the hydrogen adsorption/desorption peaks between 0.05 and 0.4 V. With the increase in the deposition cycles, the hydrogen adsorption/desorption currents gradually decrease, indicating that hydrogen adsorption is blocked by Bi adatoms.

**Figure S10.** (A) Polarization curves and (B) histograms of the specific activities at 0.5 V towards formic acid electrooxidation for different catalysts. (C) Polarization curves and (D) histograms of the specific activities at 0.8 V towards methanol electrooxidation in 0.5 M  $\text{H}_2\text{SO}_4$  + 1 M  $\text{CH}_3\text{OH}$  for different catalysts.

# Influence of alloying

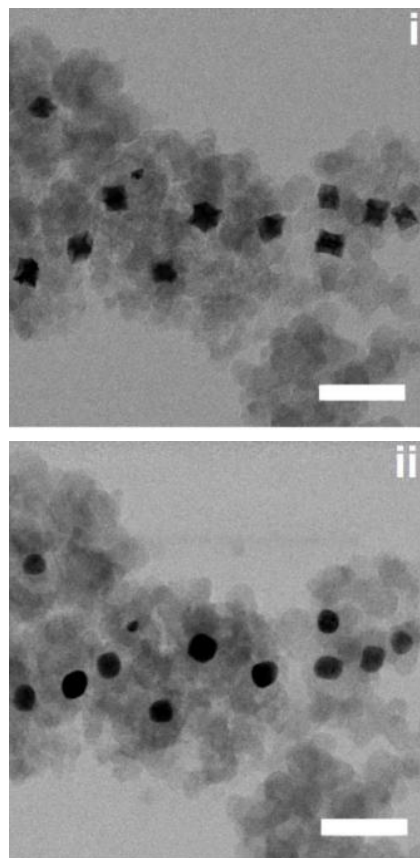


**Figure S11.** STEM images of PtNi nanoparticles i) before and ii) after thermal treatment. Scale bar 100 nm

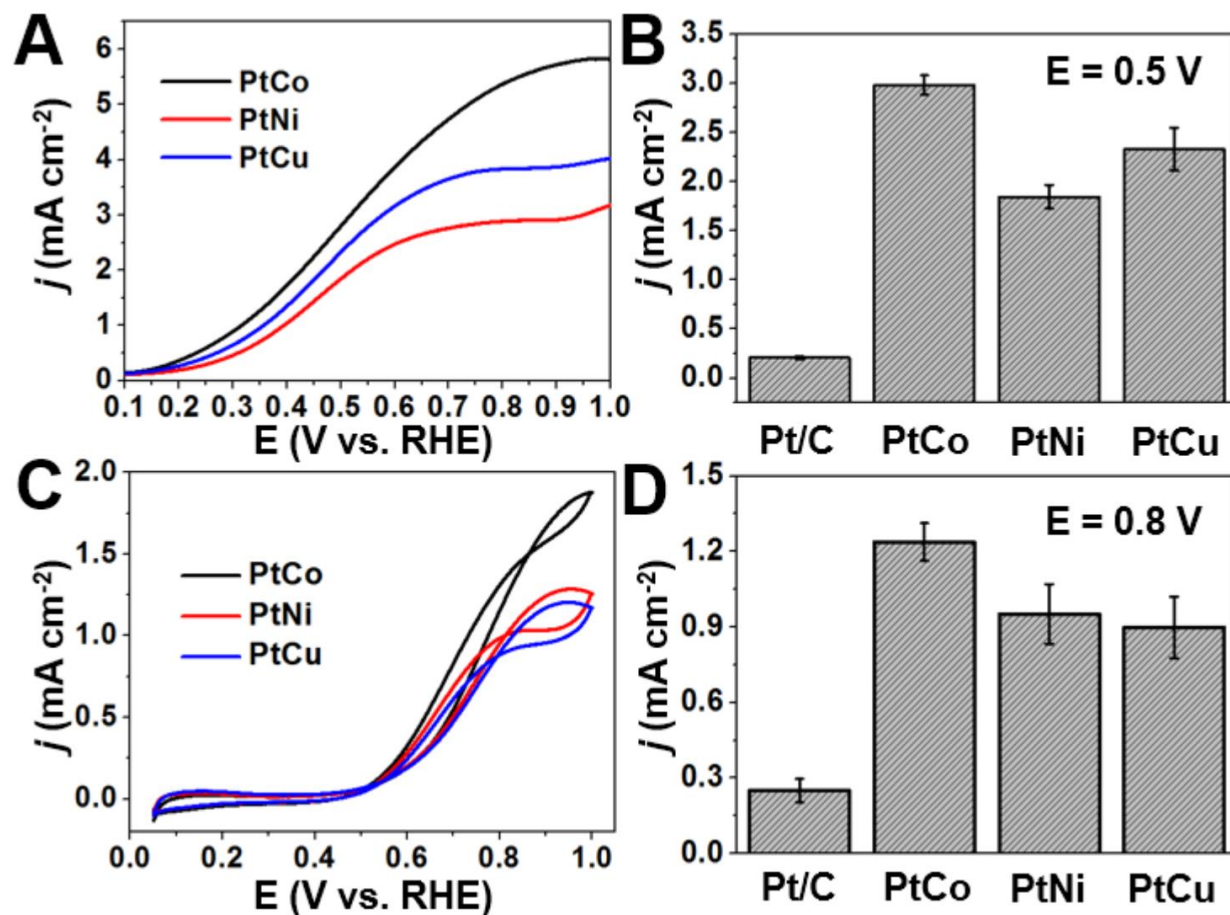


**Figure S12.** (A) Polarization curves and (B) histograms of the specific activities at 0.5 V towards formic acid electrooxidation of different catalysts. (C) Polarization curves and (D) histograms of the specific activities at 0.8 V towards methanol electrooxidation in 0.5 M H<sub>2</sub>SO<sub>4</sub> + 1 M CH<sub>3</sub>OH of different catalysts.

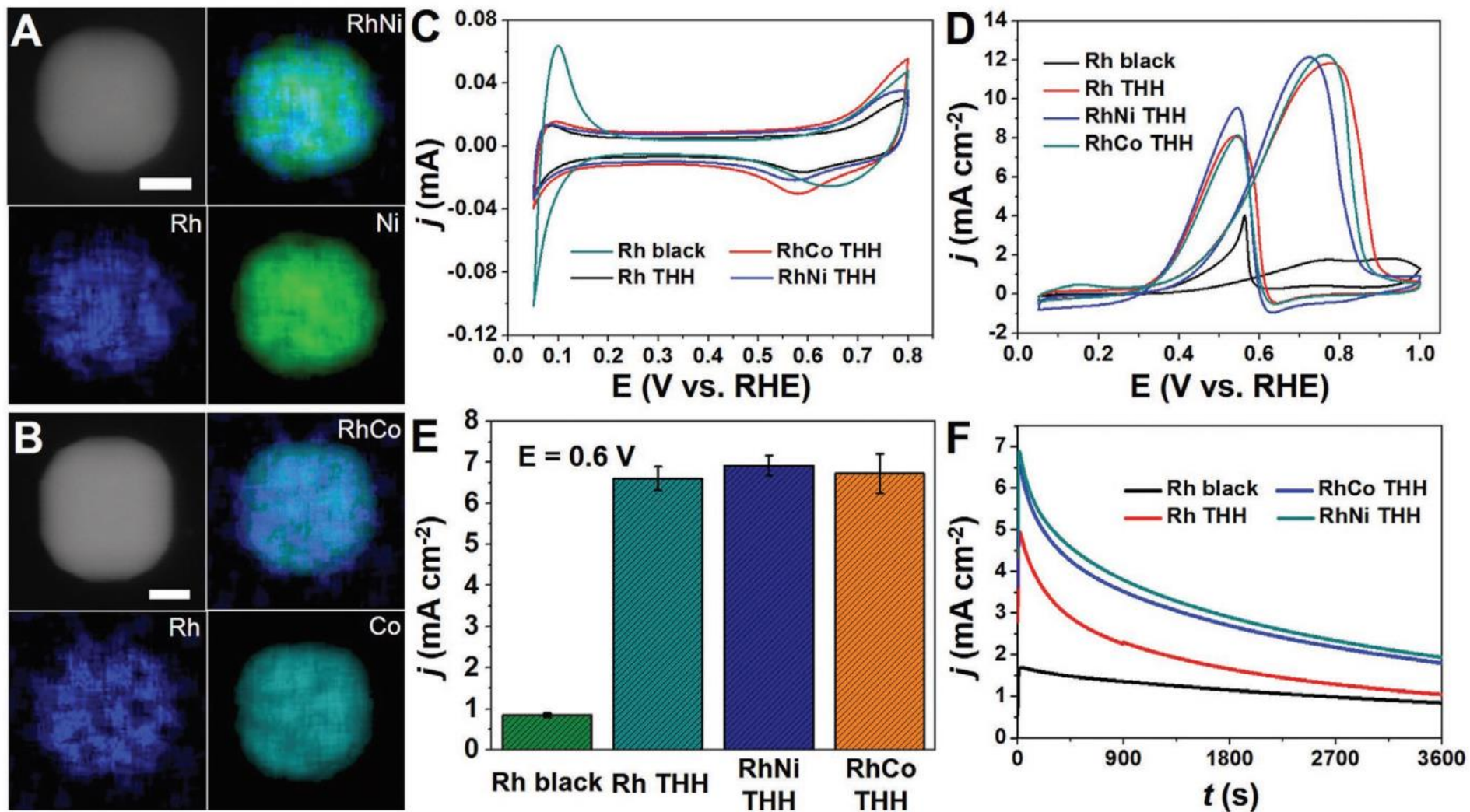


**Figure 4.** A,B) STEM images and corresponding elemental maps of RhNi (A) and RhCo (B) THH nanoparticles. C) Cyclic voltammograms of different catalysts in an Ar-saturated 0.5 m H<sub>2</sub>SO<sub>4</sub> solution. D) Polarization curves and E) histograms of the specific activities at 0.6 V of ethanol electrooxidation in Ar-saturated 0.1 m NaOH + 1 m CH<sub>3</sub>CH<sub>2</sub>OH for different catalysts. Error bars represent the standard deviation. F) Chronoamperometry curves of ethanol electrooxidation for the different catalysts at 0.6 V. Scale bars: 20 nm

# Conclusions

- ❑ Novel strategy for preparing a series of highly efficient and robust multimetallic THH electrocatalysts for typical anode reactions in fuel cells.
- ❑ Importantly, the resulting multimetallic catalysts have three features favourable for catalytic performance.
- ❑ This strategy likely can be extended to other systems (NPs containing Pt, Pd, Rh, Au, Ni, Co, and Cu synthesized with Sb, Bi, Pb, or Te modification).
- ❑ The catalyst performance can be further improved by optimizing NP size, composition, surface state, and the preparation process before transitioning to practical applications.
- ❑ Greater opportunities and flexibility in the design and discovery of high performance or low-cost electrocatalysts.

# Multimetallic High-Index Faceted Heterostructured Nanoparticles

Liliang Huang, Haixin Lin, Cindy Y. Zheng, Edward J. Kluender, Rustin Golnabi, Bo Shen, and Chad A. Mirkin\*

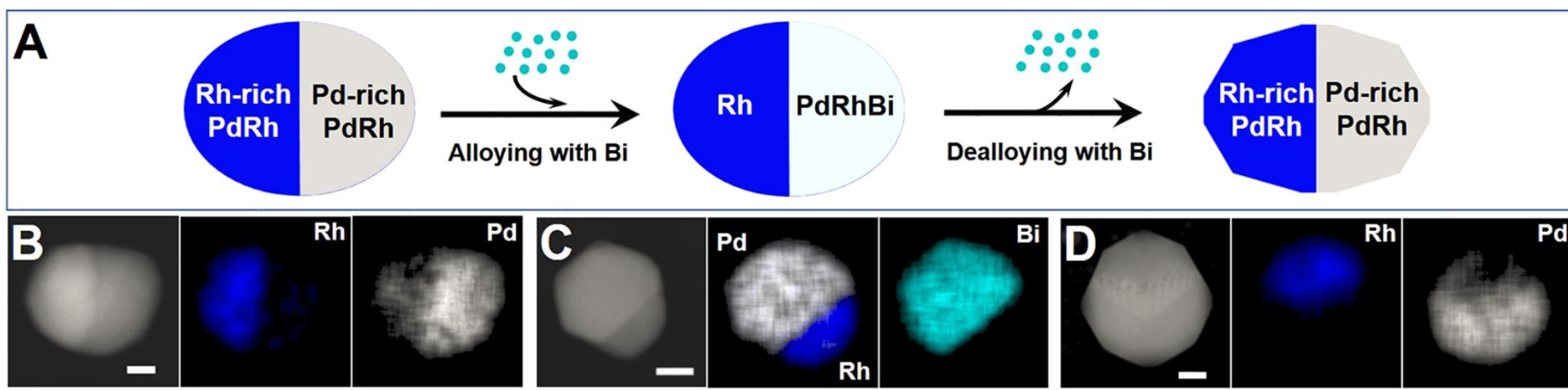


Fig: Scheme of the structural evolution of a PdRh nanoparticle during the alloying/dealloying process with Bi. STEM images and EDS elemental maps of (B) PdRh, (C) PdRhBi, and (D) PdRh THH particles.